Available online at www.sciencedirect.com
ScienceDirect
Palaeogeography, Palaeoclimatology, Palaeoecology 260 (2008) 245–261
PALAEO
www.elsevier.com/locate/palaeo

Retreat history of the Ross Ice Sheet (Shelf) since the Last Glacial Maximum from deep-basin sediment cores around Ross Island

R.M. McKay [a,*], G.B. Dunbar [a], T.R. Naish [a,b], P.J. Barrett [a,c], L. Carter [a], M. Harper [c]

[a] *Antarctic Research Centre, P.O. Box 600, Victoria University of Wellington, New Zealand*
[b] *GNS Science, P.O. Box 30-368, Lower Hutt, New Zealand*
[c] *School of Geography, Environment and Earth Sciences, P.O. Box 600, Victoria University of Wellington, New Zealand*

Received 28 May 2007; accepted 22 August 2007

Abstract

Radiocarbon-dated sediment cores from deep basins beneath the McMurdo Ice Shelf, and seasonally open water north of Ross Island, McMurdo Sound, display a characteristic succession of sedimentary facies that document the retreat of the Ross Ice Sheet at the Last Glacial Maximum to its present ice shelf configuration. The facies succession records a transition from a nearly-grounded ice sheet to open marine environments (north of Ross Island) that comprises in ascending stratigraphic order: (1) slightly consolidated, clast-rich muddy diamict dominated by basement clasts from the Transantarctic Mountains, and interpreted as melt-out from the basal layer debris proximal to a retreating grounding zone; (2) sparsely-fossiliferous (reworked diatom frustules) and non-bioturbated mud lacking lonestones, interpreted as a sub-ice shelf facies; and (3) diatom mud and diatom ooze indicative of open marine conditions with evidence of iceberg rafting. The succession in the open marine Lewis Basin north of Ross Island is similar, though the diamict is much sandier and sedimentation rates 1–2 orders of magnitude higher. We present a radiocarbon chronology from total organic carbon which implies that lift-off of grounded ice in the 900 m-deep marine basins surrounding Ross Island occurred by ~10,100 ^{14}C years BP. Following lift-off, an ice shelf was maintained to the north of Ross Island until ~8900 ^{14}C years BP. We identify a phase of accelerated retreat at that time between the Drygalski Trough and Ross Island, immediately preceding the timing of Meltwater Pulse 1b. At ~8900 ^{14}C years BP the calving line became pinned to Ross Island, significantly decoupling from the grounding line, and marking the transition from a retreating ice sheet to the development of the present ice shelf.

Keywords: Antarctica; Ross Ice Shelf; Holocene; Last Glacial Maximum; Glacimarine

1. Introduction

The Ross Ice Shelf, Antarctica, is the largest ice shelf in the world (560,000 km^2) and is fed by outlet glaciers that drain the East Antarctic Ice Sheet (EAIS) along its western margin (e.g. Denton and Hughes, 2002). However, most of the ice shelf is nourished directly by fast-flowing ice streams that drain the West Antarctic Ice Sheet (WAIS; Bindschadler, 1998). Future stability of the Ross Ice Shelf, which is coupled to the behaviour of the WAIS, has been of wide interest (Mercer, 1978) in the context of current global warming projections (IPCC, 2007). Despite calving of a 30 km-wide strip

* Corresponding author.
E-mail address: robert.mckay@vuw.ac.nz (R.M. McKay).

0031-0182/$ - see front matter © 2008 Elsevier B.V. All rights reserved.
doi:10.1016/j.palaeo.2007.08.015

of ice from its northern margin in 2000, the Ross Ice Shelf is currently considered to be stable, as the mean summer temperature is around −8 °C (Oppenheimer, 1998). However, recent glaciological evidence indicates that the Ross Ice Shelf is becoming increasingly undernourished with one of its ice stream feeders from West Antarctica stagnating and at least one other slowing down (Joughin and Tulaczyk, 2002; Joughin et al., 2005).

Fluctuations in flow velocity of the ice streams near the WAIS grounding line have been observed (Joughin et al., 2002; Bindschadler et al., 2003; Bougamont et al., 2003), and suggest that over timescales of decades to centuries ice shelves represent the most vulnerable element of the WAIS–Ross Ice Shelf system, and that their collapse could come rapidly (MacAyeal, 1992). Their demise may be the precursor to eventual collapse of the WAIS (Mercer, 1978).

Collapse of the Ross Ice Shelf could affect climate, WAIS extent, and sea level in several ways: Firstly, production of dense bottom water could be disrupted by an initial large-scale discharge of low density meltwater, reducing the production of bottom water around Antarctica. Such an effect could alter the global thermohaline ocean circulation system (Clark et al., 2002; Weaver et al., 2003; Stocker, 2003). Secondly, Earth's albedo will decrease as 560,000 km^2 of permanent ice cover is replaced with dark ocean, albeit with seasonal sea ice cover, consequently amplifying regional warming. Lastly, the exchange of heat and water vapour between the ocean and the atmosphere could lead to accelerated loss and eventual collapse of the marine-based WAIS in as little time as a few centuries, raising sea level by 5 to 6 m (e.g. Alley and Bindschadler, 2001). Of particular concern is that the fundamental behaviour of the Ross Ice Shelf is poorly understood and models on which predictions are based need to be constrained by new data (Bentley, 2004; Huybrechts, 2004), including those gathered from records of the ancient Ross Ice Shelf during the last major global warming event from the Last Glacial Maximum (LGM) ~22 Ka to present.

Between 26.5 and 19.5 Ka (LGM), the Ross Ice Shelf was grounded (Ross Ice Sheet) near the edge of the continental shelf (~Coulman Island) at approximately 700 m below present day sea level (Anderson et al., 1992; Domack et al., 1999; Bart et al., 2000), and the retreat of both grounding and calving lines since then have been reconstructed using cores collected from the open Ross Sea and ice seismic reflection profiles (e.g. Licht et al., 1996; Domack and Harris, 1998; Conway et al., 1999; Domack et al., 1999; Shipp et al., 1999). Based on a series of piston cores, Domack et al. (1999) proposed a sedimentological model describing the LGM–Holocene retreat of the WAIS (Ross Ice Sheet) in the western Ross Sea. Their lithologic succession in ascending stratigraphic order comprises: (1) Massive mud-rich, over-consolidated diamicton reflecting a sub-glacial setting; (2) a thin, stratified and loosely compacted granulated facies indicative of the glacier "sole" lift-off zone; (3) a terrigenous mud sub-ice shelf facies; (4) a siliceous mud and ooze characteristic of seasonally open marine conditions.

Radiocarbon dating of organic matter in the cores provided a chronology for post-LGM retreat of the Ross Ice Sheet that showed the grounding line withdrew from the outer Drygalski Trough to the vicinity of Ross Island between ~11 and 7 Ka ^{14}C BP (Domack et al., 1999; Conway et al., 1999). While the grounding line has continued to retreat during the Holocene, the calving line has remained pinned at Ross Island (Fig. 1).

In this paper, we examine the sedimentary evidence for Holocene stability of the McMurdo Ice Shelf, a small body of permanent floating ice at the northwest corner of the Ross Ice Shelf (Fig. 2), based on new sediment cores and oceanographic data from beneath the McMurdo Ice Shelf, and from seasonally open water immediately to the north of Ross Island. We document a Holocene retreat history of the Ross Ice Sheet, and provide a revised chronology for the timing of grounding and calving line retreat in southern McMurdo Sound. We relate these observations to the retreat history of the WAIS since the LGM.

2. Regional setting

The McMurdo Ice Shelf occupies an area of 2500 km^2 at the northwest corner of the much larger Ross Ice Shelf and is fed mainly by glaciers flowing from the Transantarctic Mountains and Ross Island and surface snow accumulation of ~0.3 m/year (McCrae, 1984). It is buttressed against the much larger Ross Ice Shelf along a shear zone extending from Minna Bluff to Cape Crozier (McCrae, 1984; Whillans and Merry, 1996; Kellogg et al., 1996), and the presence of the Ross Ice Shelf in this region allows for the survival of the McMurdo Ice Shelf. The area over Windless Bight where the cores for this study were taken is melting at the base, but is likely free of sediment (McCrae, 1984; Barrett et al., 2005). A simple calculation based on ice flow velocity (100 m/year), ice shelf thickness (70 to 150 m) and ice shelf accumulation balanced by basal melting suggests that basal glacial debris sourced even as close as Ross Island would have melted out a few

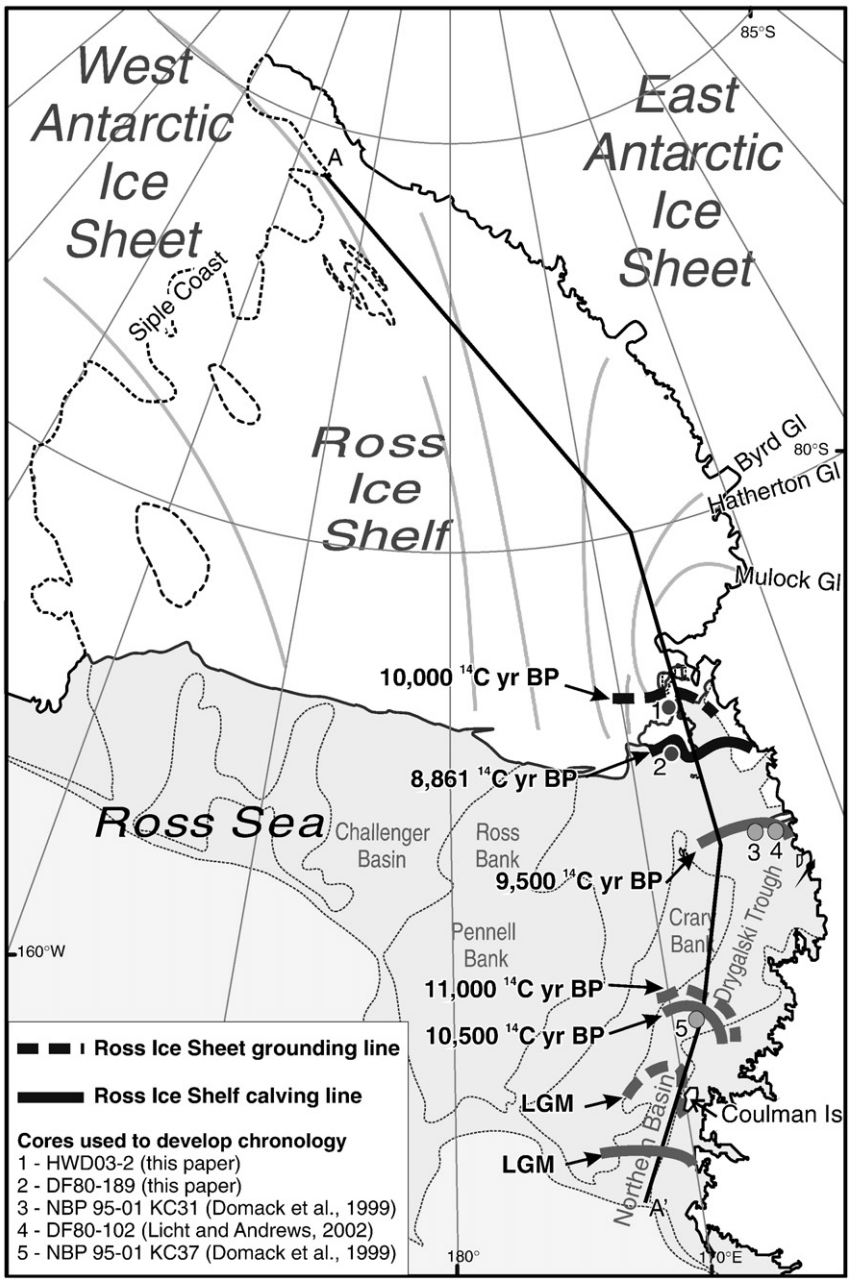

Fig. 1. Map of Ross embayment showing regional bathymetry (500 m contours), simplified modern ice flow for the Ross Ice Shelf (after Fahnestock et al., 2000), and localities mentioned in the text. Also shown is a chronology for the retreat of the Ross Ice Sheet from this study (black lines and circles) and previous workers (dark grey)––solid lines indicate the maximum position of the calving line for the Ross Ice Shelf, while dashed lines indicate the maximum position of the grounding line, including its present day position along the Siple Coast. Ice shelf extent at the LGM is poorly constrained and is based on a sedimentary hiatus observed in sediment cores (Licht et al., 1996). Transect line A-A' for Fig. 5 is also shown.

kilometers beyond the grounding line, and long before the shelf ice reached the Windless Bight core sites.

Sediment in the western Ross Sea today is accumulating primarily in north–south-trending troughs between 600 and 1200 m deep, once sites of former ice streams draining the WAIS and EAIS-sourced outlet glaciers during the Last Glacial Maximum (Hughes, 1977; Mosola and Anderson, 2006). However, 500 km south of the continental shelf edge, and 300 km south of the LGM grounding line, volcanic Ross Island is surrounded by a basin over 900 m deep, termed a "flexural moat", formed by lithospheric loading (Stern

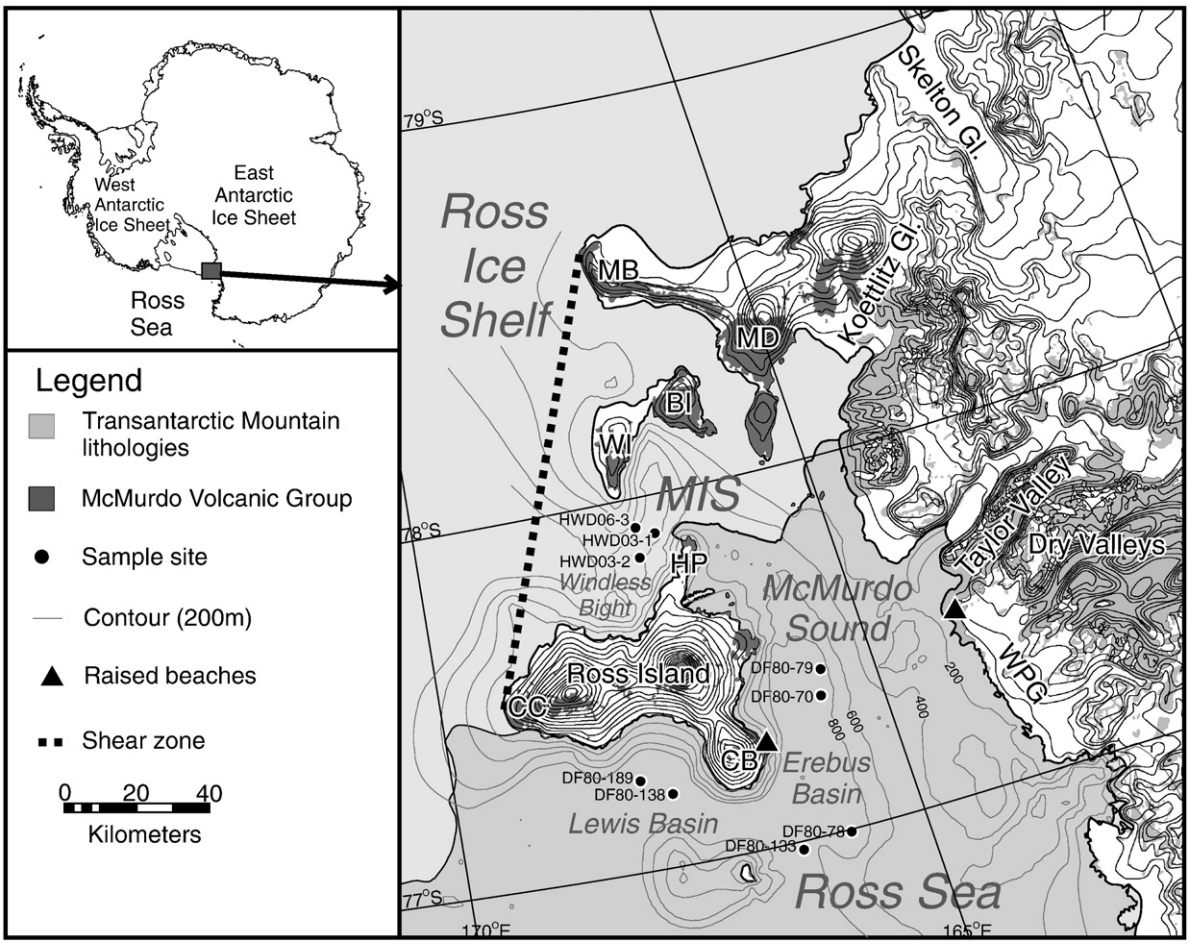

Fig. 2. Map of Ross Island region showing the core sites in this study, and localities mentioned in text. The two main provenance areas and raised beaches locations (Hall and Denton, 1999; Dochat et al., 2000) discussed in text are also shown. BI = Black Island, CB = Cape Bird, CC = Cape Crozier, HP = Hut Point Peninsular, MB = Minna Bluff, MD = Mount Discovery, WI = White Island, WPG = Wilson Piedmont Glacier.

et al., 1991; ten Brink et al., 1997; Horgan et al., 2005). The moat is interrupted only for a few kilometers southwest of Hut Point Peninsula (Fig. 2), where the sea floor rises to 600 m, accelerating the ocean current flow between McMurdo Sound and Windless Bight.

Sea floor sediment in the Ross Sea is a mix of biogenic silica (largely diatom remains from algal growth in the open ocean or sea ice), terrigenous mud carried in suspension from the adjacent continent, and sand and gravel carried by floating ice. Sediment-bearing ice can be sea ice with sand wind-blown from land, McMurdo Ice Shelf fragments from the western ablation zone with volcanic surface debris or basal debris from TAM outlet glaciers (Barrett et al., 1983). Terrigenous mud dominates the sea floor sediment throughout the Ross Sea, even though locally biogenic silica can exceed 40% in the deeper open water basins (Dunbar et al., 1985). Ice-rafted sand and gravel is widespread but forms only a few percent of sea floor sediment (Barrett et al., 1983). Sediment origin can be readily determined from mineralogy and clast composition — quartz-free dark basic to intermediate volcanic rocks come from Ross Island and the volcanoes of southern McMurdo Sound (Kyle, 1990), whereas quartz grains and granitoid or metasedimentary rocks come from the quartz-rich Cambro-Ordovician basement and overlying Beacon Supergroup strata of the Transantarctic Mountains (Craddock, 1970, Plate 13).

Diatom blooms generate frustules that settle to the sea floor largely as medium sand-sized pellets from browsing zooplankton in the open waters of the Ross Sea and McMurdo Sound (Dunbar et al., 1985). However, some of the frustules remain singular and in suspension long enough to be carried by currents beneath the McMurdo Ice Shelf. During 2003, the net current flow was from McMurdo Sound into Windless Bight with a mean speed

of approximately 7 cm/s, though there is a strong tidal influence with direction reversing and speeds reaching 22 cm/s (Robinson and Pyne, 2004). The net flow is sufficient to carry frustules and terrigenous mud, but not pellets or sand for tens to hundreds of kilometers beneath the ice (Barrett et al., 2005).

3. Methods

Three sediment gravity cores from beneath the McMurdo Ice Shelf were collected during 2003 and 2006 (Fig. 2). In addition, we analyzed six piston cores from the Erebus Basin (in McMurdo Sound) and the Lewis Basin (north of Ross Island), collected by the *USCGC Glacier* as part of Operation Deep Freeze (DF) in 1979–80 (Fig. 2). To sample beneath the McMurdo Ice Shelf, three Hot Water Drill (HWD) access holes were made through which a gravity corer was deployed. Detailed logging, sampling, and X-ray imaging of the Deep Freeze 80 cores were conducted at the Antarctic Marine Geology Research Facility at Florida State University. Core descriptions follow the terminology of Hambrey et al. (1997), and are based on visual observations, smear slide analysis, and X-radiography. Shear strength was measured on split cores using a Haake Rotovisco RV-12/500M. The vane used with the instrument was inserted 1 cm deep into the sediments and rotated. Shear strength (kPa) was measured at peak failure (Barrett et al., 2005). Detailed core logs and grain size results for the cores discussed in this paper are available in Barrett et al. (2005) and Carter et al. (2007).

Ice-rafted debris (IRD) was quantified by summing the number of grains visible on X-radiographs and exceeding 2 mm in size, in 1 cm thick horizontal bands following the method of Grobe (1987). We counted to a maximum of 10 grains in each cm-band because quantities higher than this were difficult to determine accurately as individual grains began to overlap in the X-ray image. Therefore, we arbitrarily assigned the maximum value of 10 grains >2 mm to these intervals. This readily allows for the diamicton to be distinguished from fine-grained sediment with ice-rafted debris (see Fig. 3).

Dry sieving and Sedigraph analysis determined grain size frequency distribution at 0.5 phi intervals for the sand and mud fractions (Dunbar and Barrett, 2005). Modal petrographic analysis (300+grain point count) for the 63–500 μm fraction was undertaken on grain mount thin sections. The rock fragments and minerals characterized in these counts are summarized in Table 3, and detailed results are available as supplementary data. To determine the provenance of the sand grains, individual minerals and rock fragments were grouped into those of lithologies found solely or largely in the Transantarctic Mountains and those of more local McMurdo Volcanic Group origin (Fig. 3).

The most distinctive indicator of the Transantarctic Mountains provenance is quartz, which is absent in the McMurdo Volcanic Group (Kyle, 1990), but is derived from granites and metasediments, and quartz arenite and arkosic sandstone of the Beacon Supergroup that crops out throughout the Transantarctic Mountains. Notably, rounded quartz with overgrowths can be directly attributed to Devonian Taylor Group (Beacon Supergroup) sandstones (Korsch, 1974). Pyroxene is another important provenance marker, with pigeonite being of Ferrar Dolerite origin, and augite of McMurdo Volcanic Group origin (Smellie, 1998). In the absence of cleavage, alteration or twinning, feldspars could be difficult to distinguish from the quartz, except where conchoidal fractures, undulose extinction and/or overgrowths could be seen. Distinguishing feldspar from quartz could be normally done with confidence for larger grains (>200 μm).

Bulk mineralogy was also quantified by XRD (available as supplementary data). These measurements were undertaken by R. Soong at GNS Science, New Zealand, using a Philips *X'Pert Pro X-ray* diffractometer, and quantified using *Siroquant*, a Rietveld synthesis algorithm (e.g. Taylor, 1991).

Diatom abundances and concentrations for the DF cores were determined by settling known amounts of suspended sediment using the method of Scherer (1994). For the HWD cores, most diatom concentrations were determined from aliquots, and some results were checked by settling known amounts of suspended sample in Battarbee trays (Battarbee, 1973). The results on diatom assemblages for the HWD cores are detailed in Harper and Barrett (2007). Here we focus on the relative abundance of *F. curta* as an indicator of proximal sea ice formation (e.g. Leventer, 1998; Cunningham et al., 1999), and diatom concentration as a proxy for biogenic productivity/reworking. We also note changes in the relative abundance of fossil diatom species as a proxy measure of reworking following Sjunneskog and Scherer (2005). They interpreted an increase in fossil diatom taxa in glacial diamicts relative to overlying muds in short sediment cores from the Ross Sea (Fig. 1) to be the result of reworking from a variety of older source beds.

To test for the presence of supraglacial debris that might have passed through the McMurdo Shelf at Windless Bight site, a 20-m-long ice core from near HWD03-01 was melted and filtered at 1 m intervals. The cellulose (paper) filters (2.5 μm aperture) were dissolved by acetolysis mixture (9 parts acetic anhydride, 1 part concentrated sulphuric acid). The precipitate was washed in distilled water and weighed. This weight was then combined with

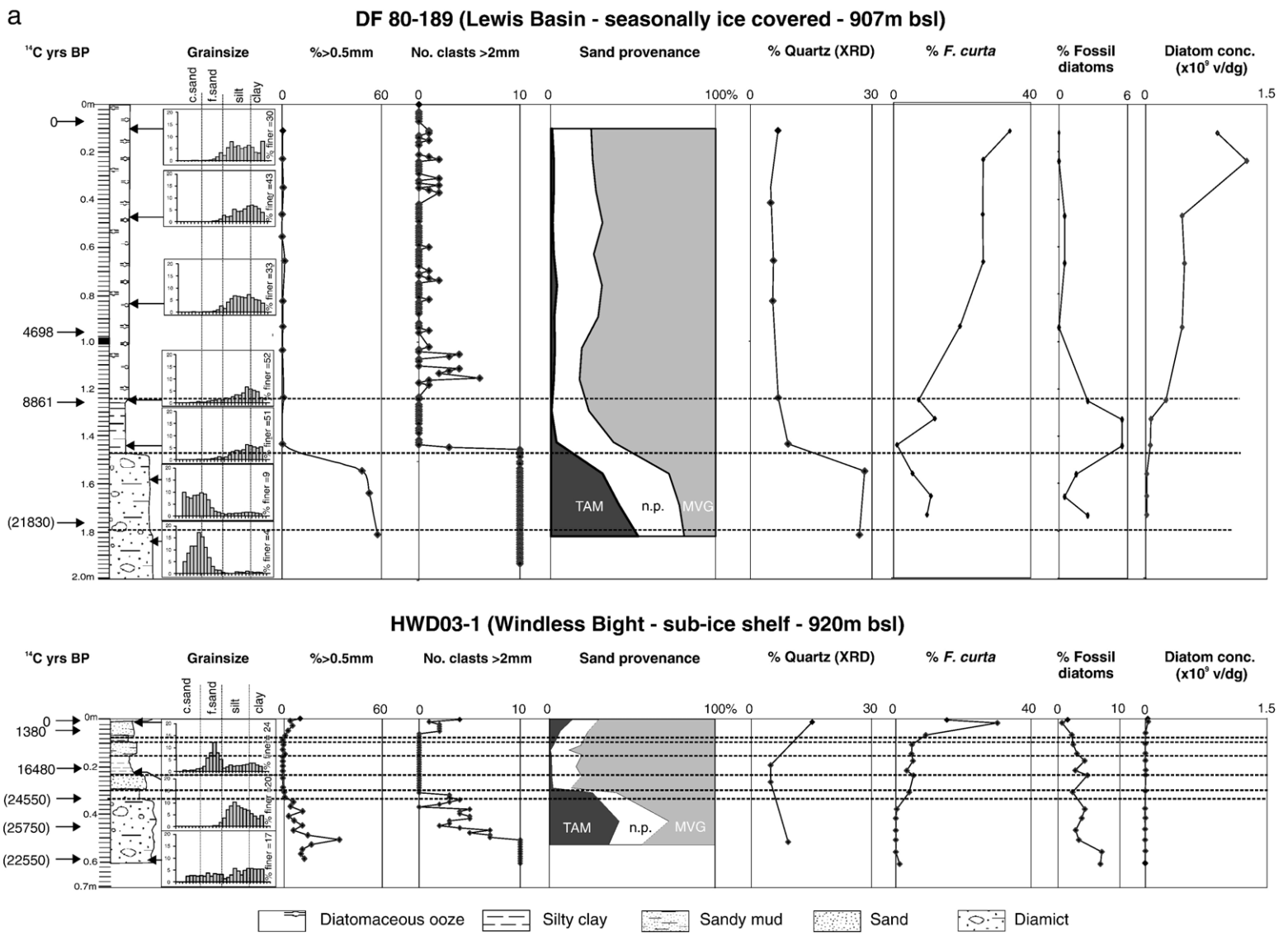

Fig. 3. a. Composite logs of DF80-189 and HWD03-1, showing corrected (where possible) radiocarbon ages, grain size histograms, % grains >0.5 mm and >2.0 mm, sand fraction (63–500 μm) provenance (TAM = Transantarctic Mountain; n.p. = no distinct provenance; MVG = McMurdo Volcanic Group), % quartz measured by XRD, and diatom abundances. Bracketed radiocarbon dates are reported ages (i.e. uncorrected). b. Composite logs of DF80-133 and HWD03-2, showing corrected radiocarbon ages, grain size histograms, % grains >0.5 mm and >2.0 mm, sand fraction (63–500 μm) provenance, % quartz measured by XRD, and diatom abundances. Bracketed radiocarbon dates are reported (uncorrected) ages.

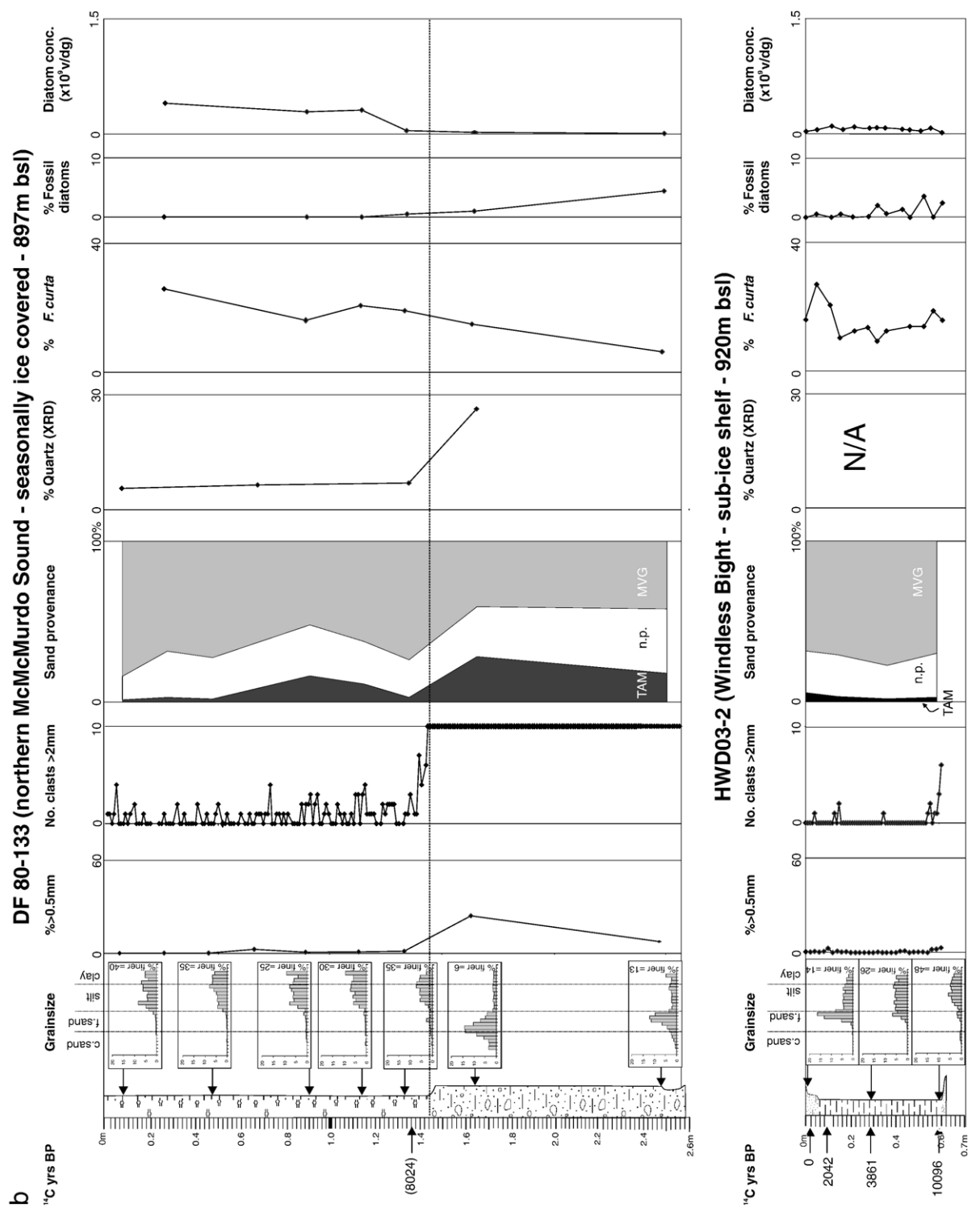

Fig. 3 (*continued*).

the snow accumulation estimates of McCrae (1984) to determine the sediment flux of supraglacial material that is passing through the ice shelf, assuming accumulation is balanced by basal melting.

Twenty-three ^{14}C ages were obtained from bulk organic carbon in acid insoluble organic (AIO) residues at the Rafter Radiocarbon Laboratory, Lower Hutt. Establishing radiocarbon chronologies for Pleistocene to recent sediments on the Antarctic margin is difficult (e.g. Domack et al., 1999; Conway et al., 1999; Licht and Andrews, 2002; Mosola and Anderson, 2006). Firstly, the marine reservoir correction (1200–1300 years) is substantially greater than for most of the world's oceans as a consequence of enhanced upwelling of "old" deep waters in the region (Gordon and Harkness, 1992; Andrews et al., 1999). Secondly, reworking of sediment containing organic matter without ^{14}C (i.e. beyond the usable limit of radiocarbon ~>50 Ka in age or "dead") appears to be significant in the Ross Sea (e.g. Licht et al., 1999). This mixing process increases the measured ^{14}C age by a proportion determined by the amount of "dead" carbon reworked and deposited with contemporaneous AIO material.

To place our chronology into context with previous studies, we have adopted the technique of Andrews et al. (1999), correcting our AIO dates by subtracting the surface ^{14}C date from stratigraphically-lower ^{14}C dates. This technique appears to give consistent results with a precision of around ±500 years (Andrews et al., 1999) for diatomaceous-rich sediments, which are abundant in the Ross Sea. However, it is less reliable for the transitional ice shelf/grounded glacial sediments, where the reworking of old carbon and a lack of primary production leads to ages that may be thousands of years older than the true age of deposition (e.g. Domack et al., 1999; Licht et al., 1998). Following the techniques reported in these earlier studies, our ages are given as both reported and corrected (Table 1). However, they are not calibrated or otherwise adjusted to calendar years.

Table 1
Reported and corrected radiocarbon (AIO) dates used in this study

Cruise/Core	Depth (m)	Lab code	Reported age (^{14}C years)	Percent modern	$\delta^{13}C$	$\delta^{14}C$	Corrected age (^{14}C years BP)	TOC (%)
DF80-78	2.24–2.26	NZA26112	22510±120	6	−23.3	−939.5	NA	NA
DF80-79	0.24–0.26	NZA25999	18613±85	10	−25.2	−902.1	NA	NA
DF80-79	1.09–1.11	NZA26000	17667±75	11	−24.3	−889.7	NA	NA
DF80-133	1.36–1.38	NZA25912	8024±35	37	−26	−635	NA	NA
DF80-138	0.06–0.08	NZA26113	26310±180	4	−24.2	−962.4	NA	NA
DF80-138	1.43–1.45	NZA26114	30930±320	2	−23.9	−978.8	NA	NA
DF80-138	2.44–2.46	NZA26111	20780±100	7	−25.9	−925.4	NA	NA
DF80-189	0.07–0.09	NZA25941	2470±35	73	−27.7	−273.7	0	1.98–2.01 [a]
DF80-189	0.96–0.98	NZA25939	7168±35	41	−26.7	−594.5	4698	1.51–1.56 [a]
DF80-189	1.27–1.29	NZA25913	11331±45	24	−25.2	−757.7	8861	0.56–1.2 [a]
DF80-189	1.76–1.78	NZA25940	21830±120	7	−16.5	−933.3	NA	0.15–0.27 [a]
HWD03-1	0.00–0.01	NZA18135	4343±55	58	−27.2	−423.9	0	0.39% [b]
HWD03-1	0.04–0.05	NZA18846	5845±35	48	−25.2	−520.3	1502	0.18% [b]
HWD03-1	0.20–0.21	NZA18136	18080±100	10	−24.9	−895.3	13737	0.12% [b]
HWD03-1	0.33–0.34	NZA18137	24550±190	5	−23.1	−953.1	NA	0.18% [b]
HWD03-1	0.45–0.46	NZA18856	25750±190	4	−22.6	−959.5	NA	0.15% [b]
HWD03-1	0.58–0.59	NZA18857	22550±170	6	−25	−939.6	NA	0.1% [b]
HWD03-2	0.01–0.025	NZA18138	2701±50	71	−26.9	−292.9	0	0.71% [b]
HWD03-2	0.09–0.10	NZA18847	4743±40	55	−25.3	−449.8	2042	0.46% [b]
HWD03-2	0.28–0.29	NZA18139	6562±45	44	−25.7	−561.6	3861	0.61% [b]
HWD03-2	0.58–0.59	NZA18140	12797±85	20	−25	−798	10096	0.36% [b]
HWD06-3	0.01–0.03	NZA25403	4675±40	56	−28	−448.4	NA	NA
HWD06-3	0.31–0.33	NZA25420	10982±60	25	−24.3	−746.5	NA	NA

Dates were corrected by subtracting the reported surface age for each core. Note, corrections are only made on muds and diatom oozes.
[a] TOC estimates from Licht et al., 1999.
[b] TOC results taken from Barrett et al. (2005).

4. Results

4.1. Stratigraphy

The core stratigraphy is summarized in Fig. 3a and b. We have focused our descriptions on the cores from beneath the McMurdo Ice Shelf (HWD03-1, HWD03-2 and HWD06-1) and from the Lewis Basin (DF80-189), where ^{14}C ages in the post-glacial sediments are in stratigraphic order and sedimentation rates are relatively constant. We have also used DF80-133 because it contains similar lithologies to the other cores. However, DF80-133 contains some core disturbance and therefore only one radiocarbon was obtained. Lithologies encountered in these cores include diamicts, muds, diatom-bearing muds and diatomaceous ooze.

4.1.1. Clast-rich sandy diamict unit

A moderately compacted diamict is present at the base of DF80-189 (1.46–1.96 m) and DF80-133 (1.47–2.47 m). It consists of poorly sorted gravel clasts in a muddy, coarse sand matrix. The gravel clasts are generally <50 mm in length, (although core diameter would not allow larger clasts to be recovered) and are a wide range of lithologies, including granite, quartz, metasedimentary, and basalt. Faceted and striated clasts are common. Undrained shear strength was not measured on the DF cores, as they have dried out during storage. However, qualitatively no sediments appeared over-consolidated. We are unable to determine a thickness for the diamict, as the cores could not penetrate any further than one meter into this unit.

Grain size (Fig. 3) is characterized by a distinct medium sand mode. Mud content is between 10 and 15%, which is low compared to the other diamicts. This relative lack of mud may have resulted from winnowing during or soon after deposition or from washing in the core tube, as there is evidence of core disturbance.

Sand grain provenance (Table 3) shows a clear Transantarctic Mountain signal (up to 50%), with common grains of rounded quartz and sandstone lithics (from the Beacon Supergroup), as well as varying proportions of microcline (from Granite Harbour Intrusives) and pigeonite (from Ferrar Dolerite). The maximum size of Transantarctic Mountain grains in this unit was 500 μm (i.e., the upper limit of the size fraction studied). XRD analysis also confirms a generally higher abundance (~25–30%) of quartz relative to the overlying units.

The diatom concentration is very low in this unit ($<8 \times 10^6$ v/g), both in DF-133 and DF80-189. The unit in DF80-133 is highly disturbed, and although this should not affect petrographic results for the 63–500 μm fraction, it may have had some influence on the diatom and grain size results. On this account we have sampled only the top and bottom of the unit in this core, with results supporting its correlation as shown with that in DF80-189. The increase in Transantarctic Mountain lithologies, higher quartz values as determined by XRD, and a general decrease in the proportion of *F. curta* also support the correlation (Fig. 3). This, combined with an age of 8020 (uncorrected) ^{14}C years BP in the overlying undisturbed mud at 1.36–1.38 m, suggests that the diamict in DF80-133 has a similar origin to that of DF80-189.

4.1.2. Clast-rich muddy diamict unit

This unit is present in sub-ice shelf cores HWD03-1 (0.31–0.62 m), and HWD06-3 (0–0.34 m). It is characterized by poorly sorted, angular to sub-rounded pebbles (generally <25 mm) in a sandy mud matrix. The clasts are of mixed lithologies, and display facets and striated faces. Like the sandy diamict, the sand grain petrology and XRD analysis show a distinct Transantarctic Mountain provenance. Grain size distribution indicates broad frequency distribution with no distinct mode and a mud content of approximately 80%. Diatom concentration is $<<10 \times 10^6$ valves per gram of dry sediment (v/g), and TOC values are consistently low at c. 0.25% (Barrett et al., 2005).

Undrained shear strength was measured at 8 to 22 kPa (Barrett et al., 2005). The base of this unit in HWD06-3 (0.32–0.34 m) is notably stiffer than overlying sediment, which suggests compaction beneath grounded ice. The shear vane could not be used in this section of the core due to the abundance of gravel clasts. In HWD03-1, Total Organic Carbon (TOC) in this unit varies between 0.10 and 0.18% (Barrett et al., 2005).

4.1.3. Silty clay unit

Directly overlying the diamicts are silty clays, although HWD03-1 includes intervals 0.05 to 0.08 m thick of fine sandy mud, and both HWD03-1 and -2 have such an interval for the upper few cm. No grains exceed 2 mm, and almost none exceed 0.5 mm (Fig. 3). Sand provenance is largely from the McMurdo Volcanic Group. Diatom concentrations are low, between 1×10^7 (HWD03-2) and 5.5×10^7 v/g (DF80-189). The assemblages observed are highly fragmented with a mixture of reworked oceanic and fossil forms (e.g. *Actinocyclus* spp., *Paralia sulcata*, *Coscinodiscus* spp. *Thalassiosira* spp., *Rouxia* spp., *Denticulopsis* spp.). The modern sea ice diatom, *F. curta*, constitutes <20% of the assemblage.

The lack of IRD or basally transported Transantarctic Mountain grains (Figs. 3 and 4) suggests deposition

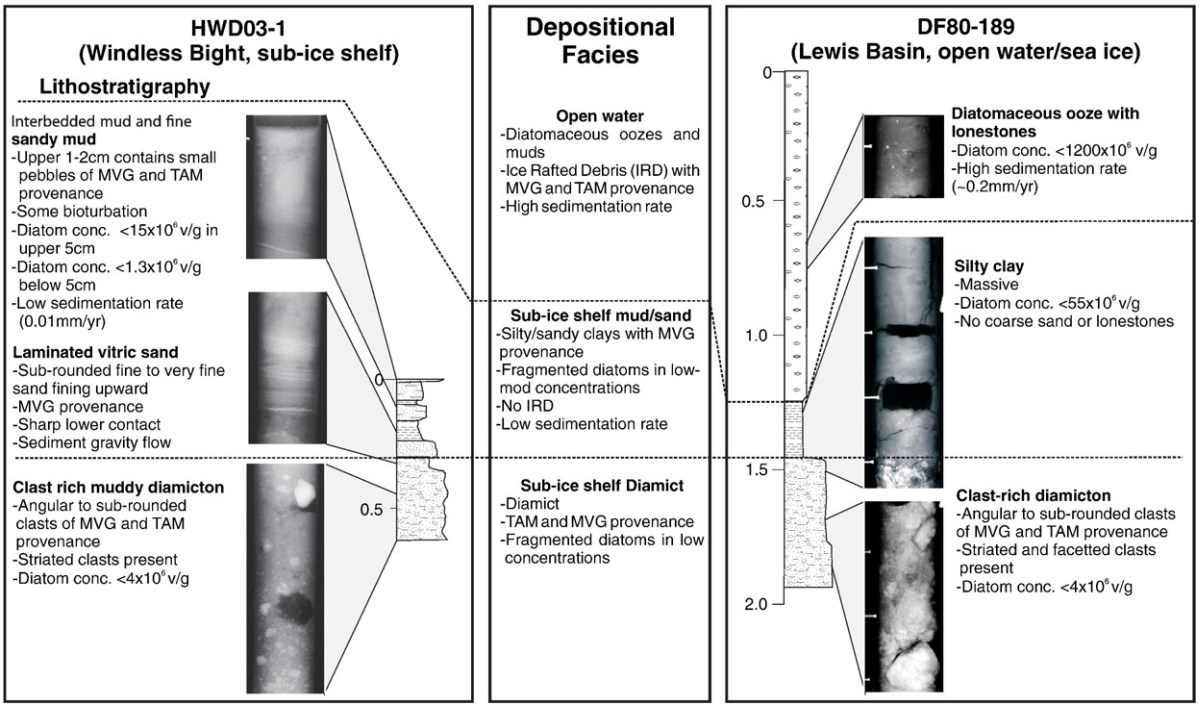

Fig. 4. Core logs, lithological characteristics, and selected X-rays of representative facies from HWD03-1 and DF80-189. Note lack of outsized sand grains in sub-ice shelf mud/sands in both cores relative to the open water diatomaceous ooze/mud in DF80-189. The laminated vitric sand in HWD03-1 is interpreted as a sediment gravity flow.

beneath an ice shelf that lacks sub-glacial debris. Sediment recovered from the surficial ice core at the Windless Bight site indicates that the present day flux of supraglacial material passing through the ice shelf at the Windless Bight site and being deposited on the seafloor is 0.05–0.55 μm/year (assuming a snow accumulation of 0.3 m/year), accounting for between 0.1 and 1% of the total sediment accumulating on the seafloor.

The maximum unit thickness is 0.60 m (HWD03-2). Radiocarbon ages (see Section 4.2) from the HWD sites imply accumulation rates of between 0.01 and 0.05 mm/year, and TOC values for this unit throughout the cores vary between 0.1 and 0.7% (Licht et al., 1999; Barrett et al., 2005).

4.1.4. Diatom mud and ooze with dispersed clasts

Diatom mud and ooze dominate the upper 1.20–1.40 m in both DF80-133 and DF80-189, taken from the seasonally open water sites of McMurdo Sound and Lewis Basin, and consist of a poorly sorted mud that is distinguished from the underlying silty clay unit by its higher concentrations of diatoms (between 2×10^8 and 1.2×10^9 v/g) which constitute >50% of the sediment. This unit is further distinguished by the presence of dispersed oversized grains >2 mm. The diatom assemblage is dominated by *F. curta*, and the fossil diatom taxa are statistically insignificant. The Transantarctic Mountain signal in the sand grain petrology fluctuates between 0 and 20%. The sedimentation rate of 0.19 mm/year is significantly higher than underlying deposits. For DF80-189, TOC values vary between 1 and 2% (Licht et al., 1999).

4.2. Chronology

Radiocarbon ages from cores DF80-78 and DF80-79 in the Erebus Basin, and DF80-138 from the Lewis Basin are not in stratigraphic order, and surface values range from 18.6 Ka to 26.3 Ka ^{14}C BP (Table 1), indicating that any sedimentation throughout the Holocene has been dominated by reworking in these cores. Ages taken from the diamict at the base of most cores varied between 20.8 and 25.8 Ka ^{14}C BP, and are not in stratigraphic order. This is to be expected, given the reworked nature of glacially deposited sediments. The fact that the ^{14}C ages are finite indicates incorporation of post-LGM carbon, and that the diamicts are glacimarine, rather than deposited by grounded ice during the LGM. In all cores, smear slide analysis indicates that organic matter is almost entirely restricted

to biogenic silica, mostly diatoms, with some sponge spicules.

Four cores provide a stratigraphically ordered chronology of the transition from regionally grounded ice to sub-ice shelf and open ocean conditions. We have focused on these cores, as they show the least reworking and the most complete facies sequence. Two are from Windless Bight (HWD03-1 and HWD03-2), one is from northern McMurdo Sound (DF80-133), and another is from the Lewis Basin (DF80-189). On account of reworking in the cores in central McMurdo Sound (DF80-70 and DF80-79) we are unable to reconstruct the timing of ice shelf retreat through McMurdo Sound itself, but we can constrain a retreat history to the immediate north and south.

The near-surface ages of these four cores lie between 2.57 and 4.68 Ka ^{14}C BP. This range is similar to those reported in previous studies from the Ross Sea (e.g. Licht et al., 1996; Domack et al., 1999; Andrews et al., 1999; Mosola and Anderson, 2006).

5. Discussion

The lithological units can be interpreted as facies with distinct biogenic and sedimentary markers for constraining the position of the grounding and calving lines of the McMurdo/Ross Ice Shelves around Ross Island. Our facies model is developed from that of Domack et al. (1999) for the Central and Western Ross Sea, with some differences.

Developing an accurate chronology of events is complicated by difficulties in ^{14}C dating Ross Sea sediments (see Methods section). In particular, the "dead" carbon in many samples through reworking of older sediment has resulted in ages representing a maximum value, rather than the depositional age of the sample. This is especially evident in McMurdo Sound. However, this effect is minimized in sediments with relatively high accumulation rates of contemporaneous carbon (e.g. Licht et al., 1999), allowing us to provide a chronology for the retreat history of the Ross Ice Sheet/Shelf that is comparable with previous studies from the marine record (e.g. Licht et al., 1996; Andrews et al., 1999; Domack et al., 1999; Licht and Andrews, 2002).

5.1. Facies model for transition from grounded ice sheet to seasonally open water

We have identified three distinct facies from which we infer the retreat of both the grounding line and calving line of the Ross Ice Shelf: 1) sub-ice shelf diamict; 2) sub-ice shelf sand and mud; and 3) open water diatom mud and ooze with IRD.

5.1.1. Sub-ice shelf diamict facies

The sub-ice shelf diamict facies is distinguished by its lithology and Transantarctic Mountain provenance. Diatom concentrations are low, and valves are usually broken. The assemblages also have relatively higher abundances of fossil and oceanic forms. We have not recovered any diamict that we believe to be deposited beneath grounded ice. However, given its unconsolidated nature, the diamict is likely to have resulted from melt-out from the basal debris zone shortly after the retreat of regionally grounded ice. We note that over-consolidation is not a prerequisite for indicating grounded ice, as sediment cores that have penetrated megascale lineations on the seafloor have recovered diamictons with low shear strengths and high water contents (Anderson, 1999). However, the ages measured from this unit range between 20.78 Ka and 25.75 Ka ^{14}C BP, which significantly postdate the 26.86 Ka ^{14}C BP age for grounded ice in McMurdo Sound (Dochat et al., 2000), and suggest some input of post-LGM carbon, which could not have occurred if the sediment were deposited beneath grounded ice. The fact that we were unable to penetrate this unit may be due to either the presence of an underlying compacted till or the presence of large clasts. Coring under the McMurdo Ice Shelf, by the ANDRILL Project, near the vicinity of HWD03-1, has revealed an over-consolidated till at 1.94 m below the seafloor underlying the less consolidated diamict that constitutes this facies in our short cores (Naish et al., 2007).

We have not included Domack et al.'s (1999) muddy pelletized gravel and sand (granulated) facies in our model. Domack et al. (1999) noted that this facies is stratified, coarsens upwards, has dropstones, and is mineralogically identical to the underlying diamict. It is inferred to be derived from the basal glacial debris zone, and represents the lift-off of the grounded ice sheet from the sea floor, with a gradual increase in sub-ice shelf reworking as the thickness of ice shelf cavity increases. None of our diamicts are stratified, suggesting that marine deposition or reworking of sediments by sub-ice shelf currents was minimal. However, the diamict from Lewis Basin and northern McMurdo Sound (DF80-133 and DF80-189) has lower mud content than the diamict at the Windless Bight site (HWD cores). The winnowing of mud during the melt-out phase may indicate a higher energy environment for Lewis Basin and northern McMurdo Sound, potentially related to submarine meltwater flows or sub-ice oceanic circulation.

5.1.2. Sub-ice shelf sand and mud facies

Sub-ice shelf sand and mud (HWD03 sites; DF80-189, 1.22–1.45 m) are distinguished by low diatom concentrations (with a low percentage of sea ice forms), a lack of grains >2 mm in diameter, a lack of sand grains derived from the Transantarctic Mountains, and a slow sedimentation rate (0.01–0.05 mm/year). However, the upper 0.05 m of HWD03-1 shows an increase in coarse sand (up to 500 μm) with a Transantarctic Mountain provenance and includes fine gravel with a mixed provenance. The presence of these grains would normally be associated with the calving line of the ice shelf. However, this site is currently beneath the McMurdo Ice Shelf, 5 km from the calving line. These grains are too coarse to be transported via sub-ice shelf currents in a settling water column. Modern sub-ice shelf currents (<22 cm/s) are only capable of laterally transporting settling fine sand grains (at most) 1 km beneath the ice shelf (Barrett et al., 2005).

Therefore, the presence of these sand grains indicates that either the ice shelf front has retreated and then re-advanced over this site, or that reworking of the older diamicts is currently taking place beneath the ice shelf. If the ice shelf had retreated past this site during the Holocene, we would expect to see a significant increase in diatom deposition and a rapid increase in the sedimentation rate (e.g. DF80-189 and DF80-133). This is not the case at either HWD03-1 or HWD03-2 (Fig. 3), indicating that there has been no period of seasonally open water above or near the site during the Holocene, despite the temperature reconstructions based on deuterium isotopes from a number of Antarctic ice cores suggesting an early Holocene optimum up to 2.5 °C warmer than present in this region (Steig et al., 2000; Masson et al., 2000). If there has been a period of calving line retreat over the site, it was almost certainly very short lived.

An alternative explanation is the reworking of exposed diamict on the seafloor from local bathymetric highs, in particular, the hummocks, drumlins, and lineations that are commonly associated with glacimarine deposition elsewhere in the Ross Sea (e.g. Shipp et al., 1999). Perhaps sub-ice shelf bottom currents increased in strength as the ice shelf front approached the site in the late Holocene. This increased flow could have winnowed fine grained material from exposed seafloor diamicts, resulting in localized slope instability.

This facies is absent in DF80-133, as grains >2 mm are persistent throughout the core. This suggests that either the ice shelf did not persist at this site for a significant length of time, or this unit has been reworked and eroded.

In HWD03-1, a distinctive dark interval (0.24–0.31 m) of well-sorted, soft, muddy fine to very fine sand (63–97% sand) with mm-scale mud laminations occurs directly above the underlying diamict facies. The sand has a sharp lower contact with load features. Petrographic analysis indicates that the sand is composted of rounded, weathered volcanic glass and lithics. This interval likely represents a series of small sediment gravity flows following grounding line retreat.

5.1.3. Open water diatom mud and ooze facies

This facies is distinguished by its higher accumulation rate (0.2 mm/year) associated with primary biogenic production. Diatom concentrations are one to two orders of magnitude higher (between 5×10^8 and 12×10^9 v/g) than for the underlying sub-ice shelf facies ($4–5 \times 10^7$ v/g) and marked by the high abundance of *F. curta*, a diatom that dominates seasonal sea ice and the adjacent water column in the Ross Sea (Leventer, 1998). Associated with this biogenic deposition is the presence of ice-rafted coarse sand and pebbles most likely derived from icebergs calving from glaciers along the Victoria Land coast and Ross Island.

5.2. Sediment provenance and ice shelf dynamics

We have identified a strong relationship between sand provenance and the position of the Ross/McMurdo Ice Shelf calving lines. During periods of glacial advance, regionally grounded ice transports large volumes of sediment derived from the Transantarctic Mountains into Windless Bight, and Erebus and Lewis basins. Transantarctic Mountain lithologies contribute up to 50% of the 63–500 μm fraction. This signal is also evident in the XRD results, with quartz generally exceeding 30% of the mineral assemblage. These results are consistent with reconstructions (e.g., Stuiver et al., 1981; Denton and Marchant, 2000) of the grounded Ross Ice Shelf transporting sediment from the Transantarctic Mountains to the south of Minna Bluff into Windless Bight, and around Cape Bird into McMurdo Sound.

The retreat of the grounding line and the development of ice shelf conditions are represented by a dramatic increase in the proportion of locally derived McMurdo Volcanic Group grains. XRD analysis suggests quartz constitutes <10% of the mineral assemblage, while Transantarctic Mountain-derived sand in the 63–500 μm fraction generally contributes <4%. However, there is potential for localized slope instability that may distort this signal. Instability may result from ice withdrawal or from the winnowing of

fine material higher up the slope due to increasing oceanic current influence. As the calving line retreated over the site, sediment provenance was still dominated by material derived from the McMurdo Volcanic Group, although there is a noticeable increase in Transantarctic Mountain lithologies (~10–15%) in the 63–500 μm fraction. These may result from poorly sorted ice-rafted debris, well-sorted wind-blown sand passing through sea ice, and/or reworking of older seafloor diamicts.

5.3. Timing and magnitude of grounding and calving retreat: Relationships to Meltwater Pulses 1A and 1B

Within the uncertainties associated with Antarctic radiocarbon ages, our corrected AIO ages are consistent with those of previous studies. However, contamination of some samples with "dead" carbon is clearly evident in intervals where ages are not in chronological order. Nonetheless, we have identified two cores where we believe the chronology is reliable. The corrected age of 8.9 Ka ^{14}C BP for DF80-189 (1.27–1.29 m), a mud with high diatom concentrations (~5.5×10^7 v/g) is likely to be robust for two reasons: (1) the age was corrected by the AIO age at 0.07 m depth (2.47 Ka ^{14}C BP), not the surface and therefore calculating the age from the surface age would result in an age >8.86 Ka ^{14}C BP. For example, using the sedimentation rates determined between 0.07 and 0.96 m depth (0.19 mm/year) to extrapolate the expected age at 0 m depth (2.05 Ka ^{14}C year), would have given a corrected age at 1.27–1.29 m of 9.28 Ka ^{14}C BP. However, we have decided to use the simple correction to 0.07 m and rounded up to 8.90 Ka ^{14}C BP for our chronology. (2) It coincides with the first signal in the diatom record of primary production, which would have provided the first significant influx of non-reworked carbon and the first signal of IRD (see Fig. 3). (3) Overlying ages are in chronological order and there is no major lithological change. This date indicates that open marine conditions were developing above this site at c. 8.9 Ka ^{14}C BP.

The underlying glacial sediments are usually low in diatomaceous material, and hence contemporaneous carbon, making ages less reliable for dating the retreat of the grounding line. However at HWD03-2, the base of 0.60 m-thick mud (which overlies a pebbly sandy mud) gives a corrected age of 10.1 Ka ^{14}C BP (Fig. 3). We believe this age is reliable given that: (1) It has a moderate diatom concentration (>10×10^6 v/g) dominated by modern Ross Sea taxa (e.g. *F. curta*, *F. obliquecostata*), (2) there is a lack of fossil diatoms which is an indicator of reworking from older sediment (Sjunneskog and Scherer, 2005); and (3) overlying sediments are comprised of a uniform lithology and the ages are in chronological order, defining a linear age–depth relationship (Fig. 3).

Thus HWD03-2 constrains the age for lift-off of grounded ice 920 m below sea level immediately to the south of Ross Island to earlier than 10.1 Ka ^{14}C BP. This is further constrained by the ~8.9 Ka ^{14}C BP age obtained for open marine conditions immediately to the north of Ross Island from DF80-189. These are included in Fig. 5, which shows our revised chronology for the retreat of the Ross Ice Sheet.

On the basis of these ages and the lithostratigraphy recorded in our cores, we postulate that the grounding and calving lines of the Ross Ice Sheet retreated at similar rates until between 8.0 and 9.0 Ka ^{14}C BP, when the calving line became pinned to Ross Island. Since then it has remained there while the grounding line continued to retreat to its present day position.

The timing of lift-off of grounded ice at Windless Bight just after 10.1 Ka ^{14}C BP is slightly earlier than previous estimates from marine sediment cores further north in the Ross Sea (e.g. Domack et al., 1999; Conway et al., 1999; Licht and Andrews, 2002), and earlier than the timing of ice retreat based on ages from proglacial lakes in the Taylor Valley at 8.34 Ka ^{14}C BP (Hall et al., 2000). These proglacial lakes are inferred to have been formed as the result of the grounded Ross Ice Sheet in McMurdo Sound. If correct, this revised chronology indicates that the retreat of the Ross Ice Sheet was more rapid and earlier than previously believed, and raises questions over its relationship to Meltwater Pulses 1A and 1B (mwp-1A and mwp-1B). Domack et al. (1999) implied that the initial post-LGM retreat of the Ross Ice Shelf grounding line from near Coulman Island at c. 11.0 Ka ^{14}C BP postdated, and was thus not the cause of, a 20 m rise in sea level between ~12.5 and 11.8 Ka ^{14}C BP (mwp-1A; Fairbanks, 1989; Bard et al., 1996). Our chronology agrees with this, but also indicates that the retreat of the grounding line from the outer Drygalski Trough to Ross Island occurred rapidly (within 1000 years), and appears to immediately precede mwp-1B, a ~10 m sea level rise that occurred between ~9.2 and 9.8 Ka ^{14}C BP (Fairbanks, 1989; Bard et al., 1996).

Considering the uncertainties associated with ^{14}C ages in the Ross Sea, and the uncertainties that surround mwp-1B, we cautiously interpret our chronology in the context of global eustatic sea level changes. Taken at face value, our chronology suggests that initial lift-off of grounded ice at Windless Bight preceded mwp-1B (Fig. 5), implying that the WAIS could have been a significant contributor to eustatic rise. Nevertheless, a northern hemisphere origin for mwp-1B, which may

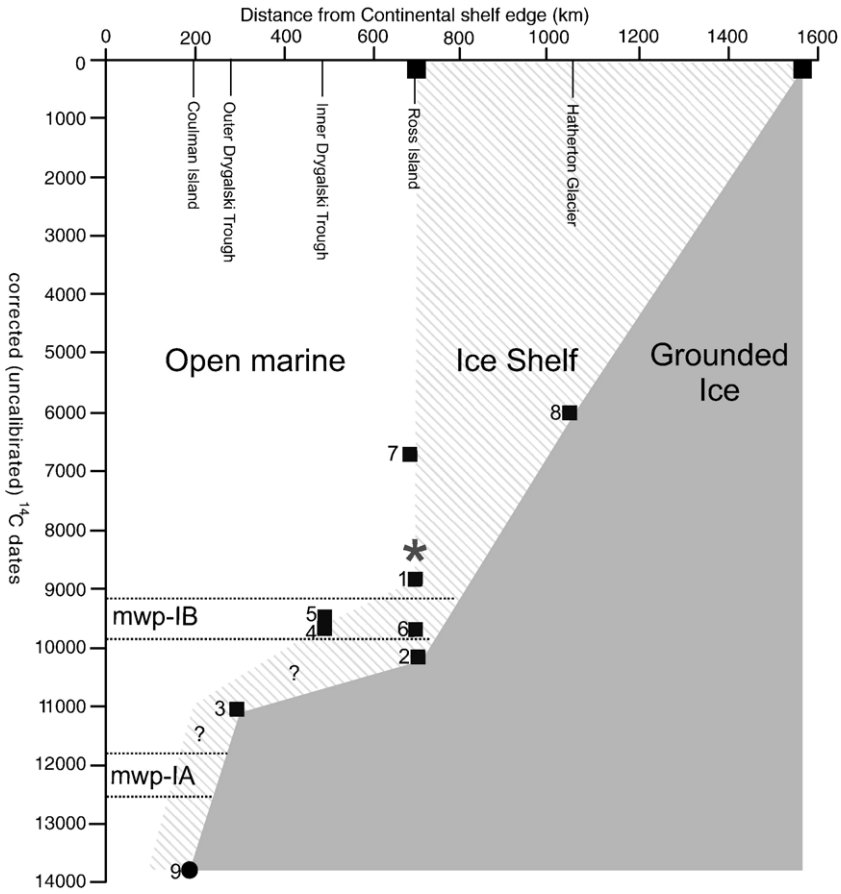

Fig. 5. The retreat history of the Ross Ice Sheet/Shelf grounding and calving line, using corrected ^{14}C dates from this study, and those of previous workers. Corrected (but uncalibrated) age ranges for Meltwater Pulse (mwp) events 1A and 1B (after Fairbanks, 1989) are also plotted. Sources for this chronology are: (1) DF80-189, AIO ^{14}C date from diatomaceous ooze with IRD, (this paper); (2) HWD03-2, AIO ^{14}C date from sub-ice shelf diatom-bearing mud, (this paper); (3) KC37, AIO ^{14}C date from sediment core (Domack et al., 1999); (4) DF80-102, AIO ^{14}C date from muddy diatom ooze, Licht and Andrews, 2002); (5) KC31 (AIO ^{14}C date from sediment core, Domack et al., 1999); (6) Oldest penguin bone at Cape Bird (Dochat et al., 2000); (7) DF80-57, oldest marine shell in McMurdo Sound (Licht et al., 1999); (8) algal date adjacent to Hatherton Glacier (Bockheim et al., 1989); (9) Inferred extent of grounded ice at the Last Glacial Maximum from seismic profiling in the Western Ross Sea (after Shipp et al., 1999), while timing of grounding line extent at 13.8 ka ^{14}C BP (Bart et al., 2000) is based on a reworked foraminifer in diamict from a sediment core (NBP9501-7) in the central Ross Sea (Licht and Andrews, 2002); *= Terrestrial evidence for grounded ice in McMurdo Sound (Hall et al., 2000).

have destabilized the marine-based Ross Ice Sheet and triggered the transition from an ice sheet to the present ice shelf, cannot be ruled out.

Our chronology also places the retreat of grounded and shelf ice from the marine basins north of Ross Island much earlier than the chronology derived from raised beaches at Cape Bird, where *in situ* penguin remains date the oldest raised beach ridge at 3.59 Ka ^{14}C BP (Dochat et al., 2000) and provide a minimum age for ice shelf retreat. However, reworked penguin bones within beach deposits at Cape Bird have been dated at 9.74 Ka ^{14}C BP (Dochat et al., 2000), implying earlier open water conditions at this location. Raised beaches along the Scott Coast in McMurdo Sound suggest deglaciation shortly before 6.5 Ka ^{14}C year BP (Hall and Denton, 1999). The raised beaches at Cape Bird and the Scott Coast can form only in the absence of an ice shelf, and therefore provide a minimum age for grounded ice retreat. The extensive reworking in DF80-78 and DF80-79 (supported by the non-stratigraphic order of the radiocarbon ages; Table 1) prevents us from determining the timing of ice shelf retreat within McMurdo Sound itself where the raised beaches are located (Fig. 2). Therefore, it is possible that an ice shelf remained in McMurdo Sound until 6.5 Ka ^{14}C BP, while open ocean conditions prevailed to the north and east of Ross Island.

The persistence of proglacial lakes in the Dry Valleys until 8.34 Ka ^{14}C BP (Hall et al., 2000) provides a maximum age for the retreat of grounded ice in McMurdo Sound, if it is assumed they were dammed by grounded

ice. However, the presence of these lakes does not indicate the extent of grounding within McMurdo Sound itself, and it is possible that localized grounding occurred along the western shoreline of McMurdo Sound until 8.34 Ka ^{14}C BP, ~1.5 kyr, perhaps as a seaward and southward extension of the modern Wilson Piedmont Glacier, after the ice lifted off the floors of the deeper basins.

6. Conclusions

- The Ross Ice Sheet grounding line retreated rapidly from the outer Dryglaski Trough to south of Ross Island between 11 and 10 Ka ^{14}C BP.
- By ~8.9 Ka ^{14}C BP, there were open marine conditions immediately to the north of Ross Island.
- The Ross Ice Shelf has been pinned to Ross Island since ~8.9 Ka ^{14}C BP while the grounding line has continued to retreat towards the Siple Coast. Its calving line has not retreated past its present position during this time, despite ice core evidence for a mid-Holocene climatic optima 1–2 °C warmer than the present (Steig et al., 1998).
- We suggest that the post-LGM retreat of the Ross Ice Sheet shifted to its contemporary ice shelf mode when the calving line became pinned by Ross Island.
- This revised chronology implies an earlier and more rapid retreat history than previously reported, and allows for the possibility that the retreat of the Ross Ice Sheet was associated with global eustatic sea level pulses.

Acknowledgements

The authors gratefully acknowledge the support and expertise of the following people and organizations. For hot water drilling, coring and drill site equipment and operation: Alex Pyne (Victoria University of Wellington), Johno Leitch (Antarctica New Zealand), and Frank Niessen, Uwe Nixdorf, and Eric Dunker from the Alfred Wegener Institut fur Polar-und Meerforschung. For support and access to the Deep Freeze 80 cores: Matt Curren (Antarctic Research Facility, Florida State University, Tallahassee). This work was financially supported by the New Zealand Foundation for Research Science and Technology (FRST) contract VIC0203 to VUW, COX0410 to GNS and subcontract to VUW, the Marsden Fund (Grant 04-GNS-010), and FRST funding (VUWX0003) for post-doctoral fellowship to GBD. Logistics support in the field was provided by Antarctica New Zealand. We are grateful to Eugene Domack and Philip Bart for comments on an earlier version of this manuscript.

Appendix A. Supplementary data

Supplementary data associated with this article can be found, in the online version, at doi:10.1016/j.palaeo.2007.08.015.

References

Alley, R.B., Bindschadler, R.A., 2001. The West Antarctic ice sheet and sea-level change. Antarctic Research Series 77, 1–11.

Anderson, John B., 1999. Antarctic Marine Geology. Cambridge University Press, UK, p. 289.

Anderson, J.B., Shipp, S.S., Bartek, L.R., Reid, D.E., 1992. Evidence for a grounded ice sheet on the Ross Sea continental shelf during the late Pleistocene and preliminary paleodrainage reconstruction. Antarctic Research Series 57, 39–62.

Andrews, J.T., Domack, E.W., Cunningham, W.L., Leventer, A., Licht, K.J., Jull, A.J.T., DeMaster, D.J., Jennings, A.E., 1999. Problems and possible solutions concerning radiocarbon dating of surface marine sediments, Ross Sea, Antarctica. Quaternary Research 52, 206–216.

Bard, E., Hamelin, B., Arnold, M., Montaggioni, L., Cabioch, G., Faure, G., Rougerie, F., 1996. Deglacial sea-level record from Tahiti corals and the timing of global meltwater discharge. Nature 382, 241–244.

Barrett, P.J., Pyne, A.R., Macpherson, A.J., 1983. Observations on the sea floor of McMurdo Sound and Granite Harbour. New Zealand Antarctic Record 5, 16–22.

Barrett, P.J., Carter, L., Dunbar, G.B., Dunker, E., Giorgetti, G., Harper, M.A., McKay, R.M., Niessen, F., Nixdorf, U., Pyne, A.R., Riesselmann, C., Robinson, N., Hollis, C., Strong, P., 2005. Oceanography and sedimentation beneath the McMurdo Ice Shelf in Windless Bight, Antarctica. Antarctic Data Series. Antarctic Research Centre, vol. 25. Victoria University of Wellington, p. 100.

Bart, P.J., Anderson, J.B., Trincardi, F., Shipp, S.S., 2000. Seismic data from the Northern basin, Ross Sea, record extreme expansions of the East Antarctic Ice Sheet during the late Neogene. Marine Geology 166, 31–50.

Battarbee, R.W., 1973. A new method for the estimation of absolute microfossil numbers, with reference especially to diatoms. Limnology and Oceanography 18, 647–653.

Bentley, C.R., 2004. Mass Balance of the Antarctic Ice Sheet: Observational Aspects. In: Bamber, J.L., Payne, A.J. (Eds.), Mass Balance of the Cryosphere. Cambridge University Press, UK, pp. 459–489.

Bindschadler, R., 1998. Monitoring ice sheet behavior from space. Reviews of Geophysics 36, 79–104.

Bindschadler, R.A., King, M.A., Alley, R.B., Anandakrishnan, S., Padman, L., 2003. Tidally controlled stick-slip discharge of a West Antarctic ice stream. Science 301, 1087–1089.

Bockheim, J.G., Wilson, S.C., Denton, G.H., Andersen, B.G., Stuiver, M., 1989. Late Quaternary ice-surface fluctuations of Hatherton Glacier, Transantarctic Mountains. Quaternary Research 31, 229–254.

Bougamont, M., Tulaczyk, S., Joughin, I., 2003. Numerical investigations of the slow-down of Whillans ice stream, West Antarctica; is it shutting down like Ice Stream C? Annals of Glaciology 37, 239–246.

Carter, L., Dunbar, G., McKay, R., Naish, T., 2007. Sedimentation and oceanography beneath the McMurdo Ice Shelf at Windless Bight, 2006. Antarctic Data Series. Antarctic Research Centre, vol. 32. Victoria University of Wellington, p. 31.

Clark, P.U., Mitrovica, J.X., Milne, G.A., Tamisiea, M.E., 2002. Sea-level fingerprinting as a direct test for the source of global meltwater pulse IA. Science 295, 2438–2441.

Conway, H., Hall, B.L., Denton, G.H., Gades, A.M., Waddington, E.D., 1999. Past and future grounding-line retreat of the West Antarctic ice sheet. Science 286, 280–283.

Craddock, C., 1970. Antarctic Map Folio Series 12, 6.

Cunningham, W.L., Andrews, J.T., Jennings, A.E., Licht, K.J., Leventer, A., 1999. Late Pleistocene–Holocene marine conditions in the Ross Sea, Antarctica; evidence from the diatom record. The Holocene, 9, 129–139.

Denton, G.H., Hughes, T.J., 2002. Reconstructing the Antarctic ice sheet at the Last Glacial Maximum. Quaternary Science Reviews 21, 193–202.

Denton, G.H., Marchant, D.R., 2000. The geologic basis for a reconstruction of a grounded ice sheet in McMurdo Sound, Antarctica, at the Last Glacial Maximum. Geografiska Annaler. Series A: Physical Geography 82, 167–211.

Dochat, T.M., Marchant, D.R., Denton, G.H., 2000. Glacial geology of Cape Bird, Ross Island, Antarctica. Geografiska Annaler. Series A: Physical Geography 82, 237–247.

Domack, E.W., Harris, P.T., 1998. A new depositional model for ice shelves, based upon sediment cores from the Ross Sea and MacRobertson Shelf, Antarctica. Annals of Glaciology 27, 281–284.

Domack, E.W., Jacobson, E.A., Shipp, S., Anderson, J.B., 1999. Late Pleistocene–Holocene retreat of the West Antarctic ice-sheet system in the Ross Sea; Part 2, Sedimentologic and stratigraphic signature. Geological Society of America Bulletin 111, 1517–1536.

Dunbar, G.B., Barrett, P.J., 2005. Antarctic Data Series. Antarctic Research Centre, vol. 24. Victoria University of Wellington, p. 55.

Dunbar, R.B., Anderson, J.B., Domack, E.W., Jacobs, S.S., 1985. Oceanographic influences on sedimentation along the Antarctic continental shelf. Antarctic Research Series 43, 291–312.

Fairbanks, R.G., 1989. A 17,000-year glacio-eustatic sea level record; influence of glacial melting rates on the Younger Dryas event and deep-ocean circulation. Nature 342, 637–642.

Fahnestock, M.A., Scambos, T.A., Bindschadler, R.A., Kvaran, G., 2000. A millennium of variable ice flow recorded by the Ross Ice Shelf, Antarctica. Journal of Glaciology 46, 652–664.

Gordon, J.E., Harkness, D.D., 1992. Magnitude and geographic variation of the radiocarbon content in Antarctic marine life; implications for reservoir corrections in radiocarbon dating. Quaternary Science Reviews 11, 697–708.

Grobe, H., 1987. A simple method for the determination of ice-rafted debris in sediment cores. Polarforschung 57, 123–126.

Hall, B.L., Denton, G.H., 1999. New relative sea-level curves for the southern Scott Coast, Antarctica; evidence for Holocene deglaciation of the western Ross Sea. Journal of Quaternary Science 14, 641–650.

Hall, B.L., Denton, G.H., Hendy, C.H., Denton, G.H., Hall, B.L., 2000. Evidence from Taylor Valley for a grounded ice sheet in the Ross Sea, Antarctica. Geografiska Annaler. Series A: Physical Geography 82, 275–303.

Harper, M.A., Barrett, P.B., 2007. A diatom record of glacial to interglacial transition beneath the McMurdo Ice Shelf, Antarctica. Diatom Research, Proceedings of the 19th International diatom Symposium.

Hambrey, M., Krissek, L., Powell, R., Barrett, P., Camerlenghi, A., Claps, M., Ehrmann, W., Fielding, C.R., Howe, J., Woolfe, K., 1997. Cape Roberts Project Core Logging Manual, Antarctic Data Series. Antarctic Research Centre, vol. 21. Victoria University of Wellington, p. 89.

Horgan, H., Naish, T., Bannister, S., Balfour, N., Wilson, G.S., 2005. Seismic stratigraphy of the Plio-Pleistocene Ross Island flexural moat-fill; a prognosis for ANDRILL Program drilling beneath McMurdo–Ross Ice Shelf. Global and Planetary Change 45, 83–97.

Hughes, T., 1977. West Antarctic ice streams. Reviews of Geophysics and Space Physics 15, 1–46.

Huybrechts, P., 2004. Antarctica: Modelling. In: Bamber, J.L., Payne, A.J. (Eds.), 2004. Mass Balance of the Cryosphere. Cambridge University Press, Cambridge, UK, pp. 491–523.

IPCC, 2007. Working Group I Contribution to the IPCC Fourth Assessment Report Climate Change 2007: the Physical Science Basis. Cambridge University Press, UK.

Joughin, I., Bindschadler, R.A., King, M.A., Voigt, D., Alley, R.B., Anandakrishnan, S., Horgan, H., Peters, L., Winberry, P., Das, S.B., Catania, G., 2005. Continued deceleration of Whillans ice stream, West Antarctica. Geophysical Research Letters 32, 4.

Joughin, I., Tulaczyk, S., 2002. Positive mass balance of the Ross ice streams, West Antarctica. Science 295, 476–480.

Joughin, I., Tulaczyk, S., Bindschadler, R., Price, S.F., 2002. Changes in west Antarctic ice stream velocities; observation and analysis. Journal of Geophysical Research 107, 32.

Kellogg, T.B., Hughes, T., Kellogg, D.E., 1996. Late Pleistocene interactions of East and West Antarctic ice-flow regimes; evidence from the McMurdo Ice Shelf. Journal of Glaciology 42, 486–500.

Korsch, R.J., 1974. Petrographic comparison of the Taylor and Victoria groups (Devonian to Triassic) in South Victoria Land, Antarctica. New Zealand Journal of Geology and Geophysics 17, 523–541.

Kyle, P.R., 1990. McMurdo Volcanic Group, western Ross Embayment; introduction [modified]. Antarctic Research Series 48, 19–25.

Leventer, A., 1998. The fate of Antarctic "sea ice diatoms" and their use as paleoenvironmental indicators. Antarctic Research Series, 73, 121–137.

Licht, K.J., Andrews, J.T., 2002. The ^{14}C record of late Pleistocene ice advance and retreat in the central Ross Sea, Antarctica. Arctic, Antarctic, and Alpine Research 34, 324–333.

Licht, K.J., Jennings, A.E., Andrews, J.T., Williams, K.M., 1996. Chronology of late Wisconsin ice retreat from the western Ross Sea, Antarctica. Geology 24, 223–226.

Licht, K.J., Cunningham, W.L., Andrews, J.T., Domack, E.W., Jennings, A.E., 1998. Establishing chronologies from acid-insoluble organic ^{14}C dates on Antarctic (Ross Sea) and Arctic (North Atlantic) marine sediments. Polar Research 17, 203–216.

Licht, K.J., Dunbar, N.W., Andrews, J.T., Jennings, A.E., 1999. Distinguishing subglacial till and glacial marine diamictons in the western Ross Sea, Antarctica; implications for a Last Glacial Maximum grounding line. Geological Society of America Bulletin 111, 91–103.

MacAyeal, D.R., 1992. Irregular oscillations of the West Antarctic ice sheet. Nature 359, 29–32.

Masson, V., Vimeux, F., Jouzel, J., Morgan, V., Delmotte, M., Ciais, P., Hammer, C., Johnsen, S., Lipenkov, V.Y., Mosley-Thompson, E., Petit, J.-R., Steig, E.J., Stievenard, M., Vaikmae, R., 2000. Holocene climate variability in Antarctic based on 11 ice-core isotopic records. Quaternary Research 54, 348–358.

McCrae, I.R., 1984. A summary of Glaciological Measurements Made Between 1960 and 1984 on the McMurdo Ice Shelf, Antarctica. Auckland: School of Engineering Report 360, Department of Theoretical and Applied Mechanics, University of Auckland, 1984.

Mercer, J.H., 1978. West Antarctic ice sheet and CO_2 greenhouse effect; a threat of disaster. Nature 271, 321–325.

Mosola, A.B., Anderson, J.B., 2006. Expansion and rapid retreat of the West Antarctic Ice Sheet in eastern Ross Sea: possible consequence of over-extended ice streams? Quaternary Science Reviews 25, 2177–2196.

Naish, T.R., Powell, R.D., Levy, R.L., and the ANDRILL science team, 2007. AND-1B Initial Science Results, ANDRILL McMurdo Ice Shelf Project. Terra Antarctica 14, 109–328.

Oppenheimer, M., 1998. Global warming and the stability of the West Antarctic Ice Sheet. Nature 393, 325–332.

Robinson, N., Pyne, A., 2004. Water Column Current Profile Analysis from Beneath the McMurdo Ice Shelf at Windless Bight and under the Sea Ice in Granite Harbour, Antarctica. Antarctic Data Series, vol. 26. Victoria University of Wellington, p. 30.

Scherer, R.P., 1994. A new method for the determination of absolute abundance of diatoms and other silt-sized sedimentary particles. Journal of Paleolimnology 12, 171–179.

Shipp, S., Anderson, J.B., Domack, E.W., 1999. Late Pleistocene–Holocene retreat of the West Antarctic ice-sheet system in the Ross Sea; Part 1, Geophysical results. Geological Society of America Bulletin 111, 1486–1516.

Sjunneskog, C., Scherer, R.P., 2005. Mixed diatom assemblages in glacigenic sediment from the central Ross Sea, Antarctica. Palaeogeography, Palaeoclimatology, Palaeoecology 218, 287–300.

Smellie, J.L., 1998. Sand grain detrital modes in CRP-1; provenance variations and influence of Miocene eruptions on the marine record in the McMurdo Sound region. Terra Antartica 5, 579–587.

Steig, E.J., Hart, C.P., White, J.W.C., Cunningham, W.L., Davis, M.D., Saltzman, E.S., 1998. Changes in climate, ocean and ice-sheet conditions in the Ross Embayment, Antarctica, at 6 ka. Annals of Glaciology 27, 305–310.

Steig, E.J., Morse, D.L., Waddington, E.D., Stuiver, M., Grootes, P.M., Mayewski, P.A., Twickler, M.S., Whitlow, S.I., Denton, G.H., Hall, B.L., 2000. Wisconsinan and Holocene climate history from an ice core at Taylor Dome, western Ross Embayment, Antarctica. Geografiska Annaler. Series A: Physical Geography 82, 213–235.

Stern, T.A., Davey, F.J., Delisle, G., 1991. Lithospheric Flexure Induced by the Load of Ross Archipelago, Southern Victoria Land, Antarctica. In: Thomson, M.R.A., Crame, J.A., Thomson, J.W. (Eds.), Geological Evolution of Antarctica. International Symposium on Antarctic Earth Sciences. Cambridge University Press, pp. 323–328.

Stocker, T.F., 2003. South dials north. Nature 424, 496–497.

Stuiver, M., Denton, G.H., Hughes, T.J., Fastook, J.L., 1981. In: Denton, G.H., Hughes, T.J. (Eds.), History of the Marine Ice Sheet in West Antarctica during the Last Glaciation; A Working Hypothesis. John Wiley & Sons, New York, NY, USA.

Taylor, J.C., 1991. Computer programs for standardless quantitative analysis of minerals using the full powder diffraction profile. Powder Diffraction 6, 2–9.

ten Brink, U.S., Hackney, R.I., Bannister, S.C., Stern, T.A., Makovsky, Y., 1997. Uplift of the Transantarctic Mountains and the bedrock beneath the East Antarctic ice sheet. Journal of Geophysical Research 102, 27,603–27,621.

Weaver, A.J., Saenko, O.A., Clark, P.U., Mitrovica, J.X., 2003. Meltwater pulse 1A from Antarctica as a trigger of the Bolling-Allerod warm interval. Science 299, 1709–1713.

Whillans, I.M., Merry, C.J., 1996. Kinematics of the shear zone between Ross Ice Shelf and McMurdo Ice Shelf, March 1996. Internal Report to Antarctic Support Associates, p. 18.